Spin Properties of Single Top Quark in All Production Modes at the LHC

E. E. Boos and A. V. Sherstnev

Skobeltsyn Institute of Nuclear Physics, Moscow State University,
119992 Moscow, Russia

Abstract

We study spin correlations of a single top quark production at the LHC. Based on an analogy of single t-quark production with polarized t-quark decay, we reproduce more simply the results by G. Mahlon and S. Parke on the existence of preferred t-quark spin axes. For the W^* and W-g fusion production modes the axes are related to the d-quark momentum. The proposed method allows to find conditions for the observation of a single t-quark polarization in production of the t-quark together with real W-boson, This process is important at the LHC. In this process spin effects are smeared out by the contribution of the diagram with a $gt\bar{t}$-vertex. A simple MC analysis shows the spin correlations in the process with subsequent top decay.

1 Introduction

The top quark is the heaviest Standard Model (SM) particle found so far, with a mass $\sim$ 175 GeV. As a consequence of so large mass the main SM decay $t \to W^- b$ proceeds without formation of hadron bound states [1]. A very interesting corollary from the fact is that hadronization effects do not smear out angular distributions of top quark decay products. So the distributions are mainly determined by the momentum and spin state of the top quark itself [2]. Single top quarks are expected to be produced highly polarized because of the (V–A) structure of the production Wtb-vertex in the SM. Spin properties of the all single top production processes are thus of special interest.

G. Mahlon and S. Parke have found that the direction of the spin of the single top quark in the W^* and W-g production processes coincides with the momentum of the down-type quark. For the W^* process the down-type quark is the $\bar{d}$-quark in the initial state [3], while in W-g fusion it is either the final spectator quark (in the majority of events), or the $\overline{d}$-quark in the initial state [3], [4].

In this talk we show that the above results have a simple explanation, if one considers single top production processes as decays of a polarized top quark considered backward in time. By considering the analogy with polarized top decay, we find conditions for significant top quark polarization in production of a single top quark together with real W-boson (tW-process). The process becomes important at the LHC collider.

In Section 2 we mention briefly all single t-quark production processes at the LHC and give a review of a spin vector method. In Section 3 we recall the results by G. Mahlon and S. Parke on top quark polarization in the W^* and W-g process and simple explanation of the results based on properties of a polarized t-quark decay. Also we analyze spin polarization for the more complicated tW-process of single top production including subsequent top decay. A Monte-Carlo study of the top quark spin effects in the tW-process is given in Section 4. Conclusions are presented in Section 5.

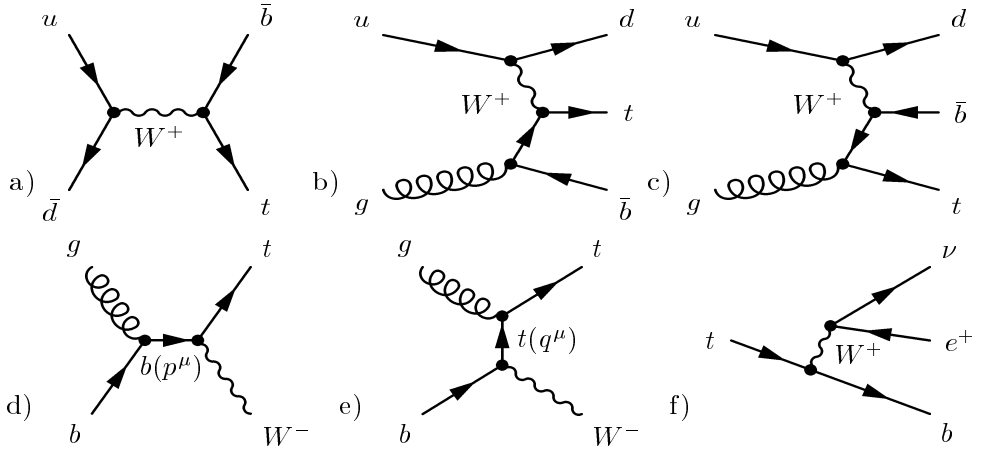

Figure 1: Typical diagrams for the W^* process (a), W-g fusion (b-c), tW-process (d-e) and LO t-quark decay (f).

2 Single Top Quark Production Processes

There are three SM processes of a single top quark production at the LHC. Some their representative diagrams[1] are shown in Fig. 1(a-e). Each of the processes may be characterized by the virtuality Q^2_W, the four-momentum squared of the participating W-boson:

- t-channel W-exchange ($Q^2_W < 0$): the characteristic diagrams are depicted in Fig. 1(b-c). This process has the largest cross section at the LHC, $\sigma = 245 \pm 27$ pb. It is referred as W-g fusion for the $2 \to 3$ diagrams shown at the figure, as well as for the $2 \to 2$ part with the b-quark in the initial state, because the initial b-quark ultimately arises from a gluon splitting $g \to b\bar{b}$. We call the diagram 1b the Wtb-diagram, because the top quark is produced in the Wtb-vertex. Respectively, the diagram 1(c) is the gtt-diagram. One should stress that for the $2 \to 2$ process there is only one Wtb-diagram.

- s-channel W-exchange ($Q^2_W > 0$): the W^* process. The characteristic diagram is depicted in Fig. 1(a). Although the process should be observable at the LHC, it has a cross section about 25 times smaller than the W-g fusion one ($\sigma = 10.2 \pm 0.7$ pb).

- Real W production ($Q^2_W = m^2_W$): tW process. A single top quark appears in association with a real W-boson as shown in Fig. 1(d-e). These diagrams are also called the Wtb-diagram and gtt-diagram, depending on the type of the t-quark production vertex. In spite of two on-shell massive particles in the final state, the tW-process rate at the LHC is significant ($\sigma = 62.0 + 16.6/-3.6$ pb). We point out the presence of two Wtb- and gtt-diagrams even for the $2 \to 2$ part of the tW-process. As it will be shown this fact leads to additional complications for the analysis of the top quark spin properties.

[1] See the complete set of contributing parton subprocesses for production on hadron colliders in [5].

The basic cross sections have been calculated at the NLO level in Ref. [6] for W-g fusion and in Ref. [7] for the W^* process, and at the LO for the tW-process in Ref. [8, 9].

The unique (V–A) structure of the SM Wtb-vertex leads to high polarization of the top quark in electroweak single top production. This statement requires more exact description of polarized states of heavy fermions themselves. Very often the discussion of spin-related observables takes place in terms of the helicity states of fermions involved [10]. Obviously, the spin state of a t-quark produced in Wtb-vertex at the LHC is not a pure helicity state. The Wtb-vertex contains a chirality projector $P_L = \frac{1}{2}(1-\gamma^5)$, but chirality and helicity eigenstates are identical only for massless particles, or in the ultra-relativistic limit. However the single t-quark is very heavy, and it is not ultra-relativistic particle at the LHC.

There is another well known description of particle spin properties, the formalism of spin vectors. It is applied for massive fermions only. The formalism is based on the invariant spin operator O_S. For a particle with four-momentum $p^\mu = (E, \bar{p})$ and mass m, it has the form $O_S = -\gamma^5\gamma^\mu s_\mu$, where s^μ is the fermion spin vector

$$s_\mu = \Big(\frac{(\bar{n}\bar{p})}{m}, \bar{n} + \frac{(\bar{n}\bar{p})\bar{p}}{m(E+m)}\Big) \ ,$$

and $\bar{n}$ is the unit 3-vector alone some direction.

The operator O_S differs from the canonical spin projection operator to the direction $\bar{n}$ derived from Noether's theorem in the quantum field theory by a unitarity transformation only. Therefore it also describes spin states of the massive fermion. If spinors $|n_4\pm\rangle$ are eigenstates of O_S with eigenvalues ± 1, then the vector $\bar{n}$ has a clear physical meaning. Spinor $|n_4+\rangle$ describes fully polarized fermion with the polarization vector $\bar{n}$ in the fermion rest frame, and $|n_4-\rangle$ is the fermion state with the polarization vector $-\bar{n}$.

With $|n_4\pm\rangle$ spinors we can introduce spin projectors $S_\pm$ which obey a condition

$$P = p^\mu\gamma_\mu + m = S_+ + S_-, \quad S_\pm = \tfrac{1}{2}(p^\mu\gamma_\mu + m)(1 \pm \gamma^5 s^\mu\gamma_\mu) \ ,$$

where P is the spin matrix of non-polarized fermion. If a process contains massive fermion in final (or initial) state, for example a t-quark, one can decompose squared matrix element of a process to the sum $|M|^2 = |M(+)|^2 + |M(-)|^2$. $|M(\pm)|^2$ depend on $S_\pm$ and describe probability of fermion production with polarization $\pm 1/2$ respectively. Obviously, existence of the extra vector s^μ gives an opportunity for more exact analysis of influence of spin on the process properties.

3 Single Top Quark Polarization

For the case of W^* and W-g fusion, G. Mahlon and S. Parke [3, 4] have found compact formulas for single top production using the spin vector formalism. For the W^* process it was shown that the expressions of the squared matrix elements $|M(\pm)|^2$ for the top quark polarized along/opposite some direction $\vec{n}_t$ in the top rest frame have a simple form [2]

$$|M(\pm, u\bar{d} \to t\bar{b})|^2 = 9g_W^4|V_{ud}V_{tb}|^2\frac{(2d\cdot t_\pm)(2u\cdot b)}{(w^2-m_W^2)^2 + (m_W\Gamma_W)^2} \ ,$$

[2] As in [3, 4] we denote the momentum of the each particle by its symbol.

where $t_\pm = \frac{1}{2}(t \pm m_t s)$. Spin vector s^μ has a form $s^\mu = (0, \vec{n}_t)$ in the t-quark rest frame.

From the 2 formulas one can see that if the polarization vector $\vec{n}_t$ points to the $\bar{d}$-quark momentum $\vec{p}_{\bar{d}}{}^*$ in the top rest frame

$$\vec{n}_{\bar{d}} = \vec{p}_{\bar{d}}{}^* / p_{\bar{d}}{}^*,$$

the squared matrix element $|M(-, u\bar{d} \to t\bar{b})|^2$ exactly equals zero. G. Mahlon and S. Parke have interpreted this result in terms of the direction of the t-quark spin coinciding with the direction of the $\bar{d}$-quark momentum ($\vec{s}_t \uparrow\uparrow \vec{p}_{\bar{d}}{}^*$).

The situation in the case of W-g fusion process is more complex. It was mentioned already long ago in the paper by Willenbrock and Dicus [11] that the W-g fusion process is dominated by the configuration where the $\bar{b}$ quark from $g \to b\bar{b}$ splitting is nearly collinear with the incoming gluon, leading to a logarithmic factor $\ln(m_t^2/m_b^2)$ in the total cross section. It is well known that these large corrections are resummed, being absorbed into the b-quark parton distribution function. The correct LO rate is obtained by summing up contributions of the $2 \to 2$ process $ub \to td$ and the $2 \to 3$ process mentioned above, with the subtraction of the first $g \to b\bar{b}$ splitting term in order to avoid double counting. The spin properties of the top quark in the $2 \to 2$ process, both in the subtracted term and in the dominant contribution of the $2 \to 3$ process coming from the Wtb-diagram, are similar in the top rest frame [4]. In all these cases the top is produced at the Wtb-vertex. The most effective spin decomposition axis is also the direction $\vec{n}_d{}^*$. But the problem of extracting the d-quark momentum direction is less obvious now, because the d-quark appears both in the initial and final states. In all cases the main spin effects are manifested in the simplest $2 \to 2$ processes with the b-quark in the initial state.

One remark is in order here. The fact that the top quark is polarized in the direction of $\vec{n}_d{}^*$ means that $|M(+)|^2 \neq 0$ and $|M(-)|^2 = 0$. For the $2 \to 3$ diagrams of the W-g-fusion (Fig. 1,b-c) the value of $|M(+)|^2$ comes from the contributions of all three parts, the Wtb, the gtt-diagrams squared and their interference. The first and third parts do not contribute to $|M(-)|^2$. The gtt-diagram in general does not produced polarized t-quark and gives nonzero contributions to both $|M(\pm)|^2$. Fortunately, $|M(-)|^2 = |M_{gtt}(-, ug \to t\bar{b}d)|^2$ is much smaller than the complete $|M(+)|^2$, which comes from the Wtb-diagram and the interference. Thus we can neglect $|M(-)|^2$ and conclude with a good accuracy that the top quark is polarized along the d-quark momentum in its rest frame.

For the tW mechanism of a single top production large corrections from the soft b-quark region also are resummed by introducing the b-quark distribution function. The $2 \to 2$ contribution with the b-quark in the initial state dominates the production rate. Therefore top spin properties can be studied by considering the $2 \to 2$ process. However, in contrast to the W-g fusion case, the gtt-diagram contribution is significant here and the corresponding diagram appears already in the $2 \to 2$ process, see Fig. 1(d-e). The situation with top polarization in the tW-process thus requires special consideration.

In order to understand t-quark spin properties in the tW-process it is useful to look at the above results for the W^* and W-g fusion processes from a different point of view. The main point of the our approach is properties of polarized top quark decay. The diagram of the LO t-quark decay, see Fig. 1(f) is topologically equivalent to the diagram for W^* process and to the $2 \to 2$ part ($ub \to td$) of the W-g fusion (it reproduces the main features of the top spin properties in the complete W-gluon fusion as we mentioned). The

decay matrix element is the same as that for production, and these processes differ only in the kinematic region over which they are integrated to get the decay width and the cross section. So the two single top production processes can be considered as a corresponding top decay backward in time. The analogue of the d-quark in top decay $t \to l^+\nu_l b$ is the charged lepton, since in the SM both the d-quark and the charged lepton are the down components of the electroweak doublets. Therefore the properties of the charged lepton from the decay should be similar to those of the d-quark.

The polarized t-quark decays have been investigated many times both in LO and NLO [2], [10, 12, 13]. The main result concerning e^+ is that it is the best spin probe of the t-quark polarization [12]. The angular distribution of the positron from the decay of the top quark polarized along some axis $\vec{n}$ in the t-quark rest frame is

$$\frac{1}{\Gamma}\,\frac{d\Gamma(\vec{s}_t \uparrow\uparrow \vec{n})}{d\cos\theta} = \frac{1+\cos\theta}{2}\ ,$$

where θ is the angle between the t-quark spin direction $\vec{n}$ and the momentum of e^+. If the direction of the top spin vector $\vec{n}$ coincides with the direction of $\vec{p}_{e^+}$ ($\theta = 0$), we get 1 in the distribution and on the contrary 0 for the opposite direction. In other words, this means that for an arbitrary top polarization state along some direction, only the state with the projection along the positron momentum direction contributes to the decay.

One should stress that the existence of a preferred spin axis is related with the (V–A) structure of the Wtb-vertex. This situation is similar to the properties of a neutrino. A chiral projector P_L cuts out the left helicity neutrino. The t-quark is the massive particle and its helicity and chirality states do not coincide. However, for the top the (V–A) Wtb-vertex leaves only the one spin projector of the t-quark in the non-polarized spin matrix $P = p^\mu\gamma_\mu + m$. The interpretation is easiest in the t-quark rest frame, where $\vec{s}_t \uparrow\uparrow \vec{n}_{e^+}{}^*$.

Now returning to the $2 \to 2$ production processes like $u\bar{d} \to t\bar{b}$ (W^*) or $ub \to td$ (W-g fusion) and keeping in mind the analogy between the positron and the d-quark we immediately conclude that the top quark is produced in a definite spin state with the top spin direction in its rest frame being along the $\bar{d}$ or d quark momentum direction.

Also it becomes obvious that after production of t-quark in a definite spin state only the projection of its spin state along the $\vec{p}_{e^-}$ direction in the top rest frame contributes. Thus the overall matrix element squared, including top production and decay, is proportional to $1 + \cos\theta^*_{e^+,d}$, where $\theta^*_{e^+,d}$ is the angle between the momenta of the e^+ and the d (or $\bar{d}$)-quark in the top rest frame. The corresponding distribution has the form:

$$\frac{1}{\sigma}\frac{d\sigma}{d\cos\theta^*_{e^+,d}} = \frac{1+\cos\theta^*_{e^+,d}}{2}$$

This result exactly reproduces the discussed result by G. Mahlon and S. Parke and corresponds to the highest possible spin correlation between production and decay. Finally, the best variable for experimental analysis of the t-quark spin properties is $\cos\theta^*_{e^+,d}$.

Although the tW process, like the W^* process or the W-g fusion part of the process with a initial b-quark, is of the $2 \to 2$ type, there are two diagrams, see Fig. 1(d-e), and one of them is of the gtt-type. As we mentioned, in contrast to the W-g fusion, the contributions of both these two diagrams are comparable in rate. We can not simply remove one of the diagram, since only together they form a gauge invariant set of diagrams.

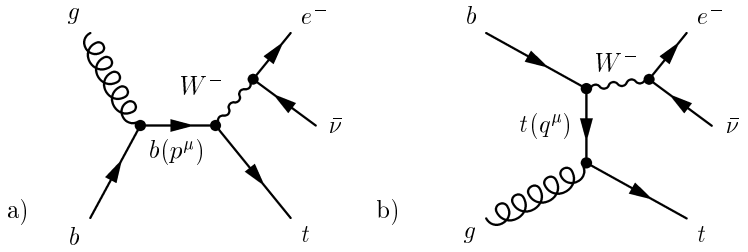

Figure 2: Diagrams of tW-process with decay of W-boson $W^- \to e^+\nu$

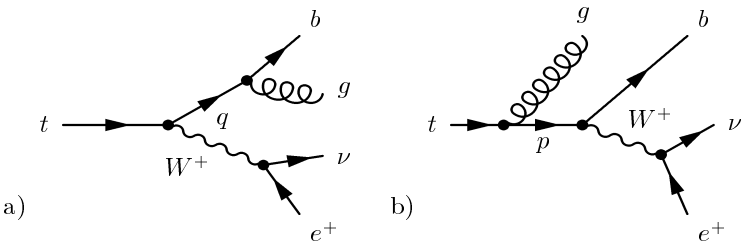

Figure 3: Diagrams of the decay $t \to b\, e^+\nu + g$

Let us consider how the analogy with the top decay helps in this case. If we consider the decay of W-boson of final state of the tW process into leptons we get the diagrams presented in Fig. 2. They are topologically equivalent to the diagrams of top quark decay with radiation of an additional gluon $t \to be^+\nu + g$ (Fig.3) which is simpler to analyze.

Let the axis for the top spin decomposition be the direction of the positron momentum produced in the W-boson decay, $\vec{n}_e{}^*$. Then one can easily check that the contribution of the Wtb-diagram squared to the top quark spin down configuration $|M_{Wtb}(-, t \to be^+\nu + g)|^2$ and the contribution of the Wtb–gtt interference diagrams $|M_{Wtb*gtt}(-, t \to be^+\nu + g)|$ equal to zero exactly in the same manner as it was for the W^* process. However, the contribution of the gtt-diagram squared $|M_{gtt}(-, t \to be^+\nu + g)|^2$ does not vanish. It turns out that the contribution for polarized t-quark decay has a simple symbolic form

$$|M_{gtt}(-, t \to be^+\nu + g)|^2 = \frac{2\, g_s^2\, g_W^2 |V_{tb}|^2}{(w^2 - m_W^2)^2 + (m_W \Gamma_W)^2} \frac{1}{(t \cdot g)^2} (b \cdot \nu) \Big[m_t E_e^* E_g^{*2} (1 - \bar{n_e^*} \bar{n_g^*})^2 \Big] ,$$

where E_e^*, E_g^*, $\vec{n}_e{}^*$ and $\vec{n}_g{}^*$ are the energies of the e^+ and gluon and the directions of their 3-momenta in the top rest frame. If the direction of the emitted gluon gets closer to the $\vec{n}_e{}^*$ in the top quark rest frame, or if the energy of the gluon gets closer to zero, the gtt-diagram contribution, where $\vec{s}_t \uparrow\downarrow \vec{p}_e{}^*$, goes to zero as well. In the limit $\cos\theta^*_{e^-,g} \to 0$ the top quark will be produced with a definite spin direction along the positron momentum.

Now let us turn to the tW production process and the analogy with the radiative decay. From the above considerations it follows that in production of t-quark in tW-process the top quark spin in its rest frame approaches 100% polarization along the momentum of the produced electron in the case when the electron momentum approaches the direction of the gluon. The same happens in the limit of zero gluon energy.

To get the cleanest top spin state, one should thus require the variable $\cos\theta^*_{e^-,g}$ to be as close as possible to unity. One can also apply a cut on upper bound of the gluon energy in the top rest frame. We have found from MC studies that an excellent variable for a cut is a combination of these two quantities, $X_{g,e^-} = E^*_g(1 - \cos\theta^*_{e^-,g})$.

Now if one considers the subsequent top quark decay, we know already that only those projections of the top spin state contribute to the top decay which coincide with the direction of the positron from the top decay. Therefore, from our considerations it follows that a good variable to probe spin properties of the top quark in the tW-process is $\cos\theta^*_{e^-,e^+}$ where the electron comes from the W-boson decay produced in association with top, and the positron comes from the top decay.

4 Monte-Carlo Results

There are 4 modes to search for the tW-process, depending on the decay channels of the t-quark and W^-–boson. Taking into account the t-quark spin, they are not equivalent.

dilepton channel: top quark (W-boson from top decay) and W^--boson decay to leptons. One can determine easily the directions of the lepton momenta. However, finding of the top quark rest frame is a problem because of the two neutrinos in the final state. 6 components of the neutrino momenta are unknown variables here. One gets only 5 equations: 2 equations from the measured missing P_T, and three ones from the 3 known masses, M_t and two M_W. An additional condition can be obtained from the simultaneous measurement of the semileptonic mode with hadronic top decay, and consequently a normalization of the leptonic mode. However the accuracy of such procedure needs to be studied in detail. Also the production rate decreases because of two small branching ratios $Br(W \to l\nu_l) = 2/9$ ($l = e$ or μ), and 1/3, if one includes τ in the analysis.

t-leptonic channel: top quark decays to leptons, W-boson – hadronically. Because of the analogy between the d-quark and the e^+ discussed above, the variable used for top spin analysis is the angle between e^+ from the top decay and the d-quark from the W decay. This mode also has a problem of the reconstruction of the t-quark rest frame, since one should extract the longitudinal part of the neutrino momentum solving the equation for the W-boson mass. Moreover, one needs to separate the d-quark jet from the u-quark jet from the decay $W^- \to d\bar{u}$ which is very problematic.

W-leptonic channel: top quark decays to jets and W-boson – to leptons. In contrast to the t-leptonic mode, the top quark rest frame could be easily extracted here, but the problem of a separation of the $\bar{d}$-quark jet in the t-quark decay remains.

hadronic channel: Although this process does not have troubles with the top and W mass reconstruction the problem of d and $\bar{d}$ jet separation from the corresponding $\bar{u}$ and u jet remains and leads to additional uncertainties. Also the QCD background is very large in this case.

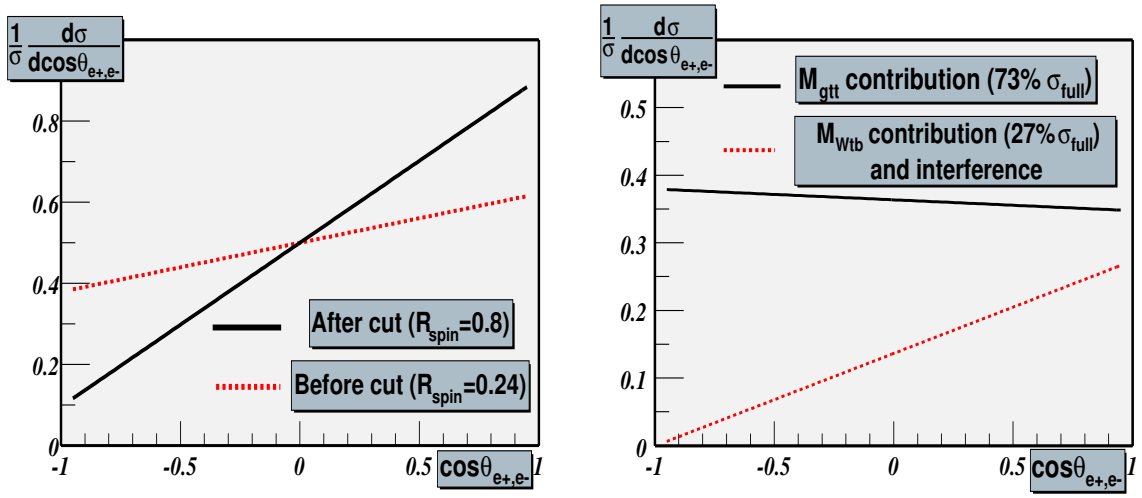

Figure 4: The normalized distributions $d\sigma/d\cos\theta^*_{e^+,e^-}$ for the tW-process (dashed line – without cuts, solid line – cut $X_{g,e^-} < 110$ GeV) and $d\sigma/d\cos\theta^*_{e^+,e^-}$ for contributions of different diagrams (right).

The complete MC analysis of the top spin properties in the tW-mode is a complicated problem and it is beyond the scope of this paper. We present only some illustrative MC results for the dilepton channel, ignoring for the moment the above problems and contributions of backgrounds. The detailed MC analysis is in progress now. The events are generated by the program package CompHEP [14] for a pp initial state at the nominal LHC energy, $\sqrt{s} = 14$ TeV with CTEQ5M1 structure functions.

The normalized distribution $d\sigma/d\cos\theta^*_{e^+,e^-}$ for the tW-process without cuts is shown in Fig. 4(left) by dashed line. As we explained, if one applies cuts on the variables $\cos\theta^*_{e^-,g}$ or E^*_g in the top quark rest frame the degree of t-quark polarization of the event sample has to increase. The above proposed best variable here is the combination of the angle and gluon energy, of the form $X_{g,e^-} = E^*_g(1-\cos\theta_{e^-,g^*})$. If the variable X_{g,e^-} is small enough, the gtt-diagram contribution is also small. The solid curve in Fig. 4(left) demonstrates a much higher spin correlation after the cut $X_{g,e^-} < 110$ GeV is applied.

It is useful to analyze the spin asymmetry R_{spin}, which is determined from the formula

$$\frac{1}{\sigma}\frac{d\sigma}{d\cos\theta^*_{e^+,\vec{s}}} = \frac{1 + R_{spin}(\vec{s})\cdot\cos\theta^*_{e^+,\vec{s}}}{2}$$

and changes between -1 to 1 for different spin axes. For a chosen spin axis $\vec{s}$ along the electron momentum direction one can express the value of the spin asymmetry as $R_{spin} = (y(1) - y(-1))/(y(1) + y(-1))$, where $y(x) = d\sigma/d\cos\theta^*_{e^+,e^-}$ and $x = \cos\theta^*_{e^+,e^-}$. If top quark would be fully polarized along the n_{e^-}, direction the spin asymmetry R_{spin} would be equal to 1.

For the tW-process $R_{spin} \approx 0.24$. It is so small because of the influence of the gtt-diagram. The individual diagram contributions in the t'Hooft-Feynman gauge are shown in Fig. 4(right). Although the contribution of the Wtb-diagram is large, the interference

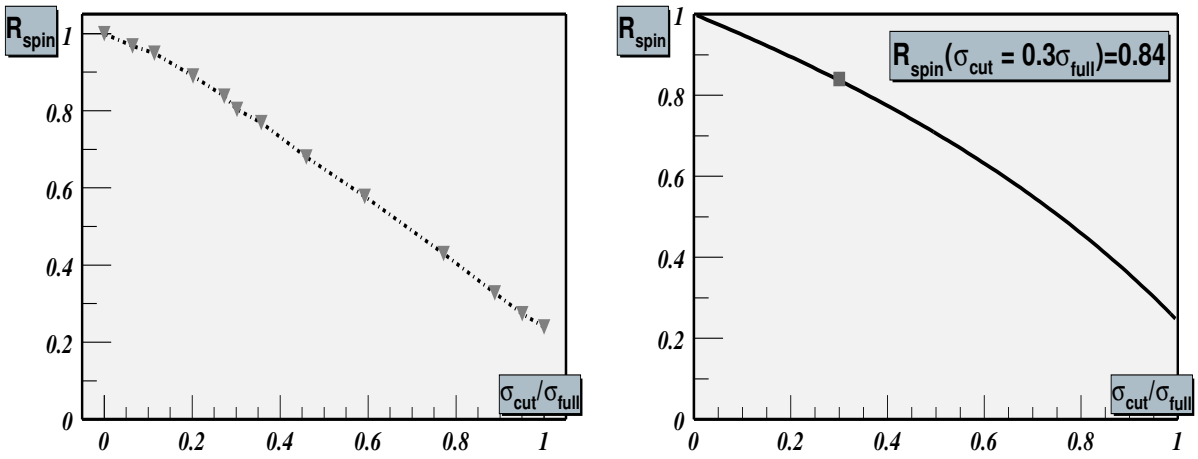

Figure 5: The spin asymmetry R_{spin} vs. the fall of the cross section for the tW-process with the X_{g,e^-} cut (left) and the $\cos\theta^*_{e^-,e^+}$ cut (right).

between Wtb and gtt-diagrams is destructive and leads to a cancellation in the angular distribution. Therefore the gtt-diagram gives the largest contribution.

As we explained above, in the limit $X_{g,e^-} \to 0$ the $R_{spin} \to 1$. In Fig. 4(left) the normalized angular distribution demonstrates the increase of R_{spin} from 0.24 to 0.80, if a proper cut on X_{g,e^-} is applied. With the cut tW-process cross section drops by a factor of 3. The dependence of R_{spin} with the cut on the cross section is shown in Fig. 5(left).

To increase of the R_{spin} we can also use the properties of the distribution $d\sigma/d\cos\theta^*_{e^+,e^-}$ itself. In Fig. 4(right) one can see that the distribution of events from the Wtb-diagram plus the interference has a peak near $\cos\theta^*_{e^+,e^-}$=1. These events correspond to polarized t-quarks along the e^- momentum. The distribution $d\sigma/d\cos\theta^*_{e^+,e^-}$ of events with the opposite top quark polarization has a peak near $\cos\theta^*_{e^+,e^-} = -1$. The contribution from the gtt-diagram is almost flat, which means it gives almost equal numbers of events with both top quark polarizations. Thus, if we cut out the region of $\cos\theta^*_{e^+,e^-}$ close to -1, a significant fraction of the events with the opposite spin configuration will be removed. Fig. 4 shows the increase of R_{spin} depending on the ratio of cross section after the $\cos\theta^*_{e^+,e^-}$ cut to the full one. In practice in order to get an event sample with higher top polarization one can use cuts on both variables X_{g,e^-} and $\cos\theta^*_{e^+,e^-}$ simultaneously.

5 Conclusions

In our talk a close relation between spin properties in a single t-quark production and in polarized t-quark decay has been pointed out. Since e^+ in top decay $t \to be^+\nu_e$ is the best probe of the top spin and because of the analogy between the e^+ and the d-type quark, one can conclude that the t-quark spin in each event is directed along the d-type quark momentum in the top quark rest frame. This is the direction of the initial $\bar{d}$-quark for the W^* process, and the dominant direction of the final d-quark for the W-g fusion process. Also it becomes obvious that the best variable to observe top spin correlations between

the top production and decay is the angle between momentum of this d-type quark in the production and the charged lepton (or d-quark) from the top decay in the top rest frame.

Spin properties of the t-quark in the tW-process are more complicated. The diagram with the top production in the gtt-vertex contributes with a significant rate in contrast to the two above processes. The analogy of the tW production to radiative polarized top decay allows to find kinematic variables, e.g. X_{g,e^-} and $\cos\theta^*_{e^+,e^-}$, to reduce events with opposite polarized t-quarks. Cuts on the variables select events with t-quarks produced with the spin vector close to the direction of the charged lepton or the d-quark momentum from the associated W decay. The cuts thus can raise the observed spin asymmetry R_{spin} in the process. We present a Monte-Carlo analysis only for the dilepton channel and at the parton level for final states. More realistic Monte-Carlo generation taking into account hadronization, identification of particles, and other effects is in progress.

6 Acknowledgments

The authors are grateful to G. Belanger and F. Boudjema for useful discussions. This research was supported in part by CERN-INTAS grant 99-0377, INTAS grant 00-0679, and RFBR grant 01-02-16710. E.B. thanks the Bessel Research Award of the Humboldt Foundation.

References

[1] I. Bigi et al., Phys. Lett. **B181** (1986) 157.

[2] M. Jeżabek and J.H. Kühn, Phys. Lett. **B329** (1994) 317.

[3] G. Mahlon and S. Parke, Phys. Rev. **D55** (1997) 7249.

[4] G. Mahlon and S. Parke, Phys. Lett. **B476**, (2000) 323.

[5] A.P. Heinson, A.S. Belyaev, and E.E. Boos, Phys. Rev. **D56** (1997) 3114.

[6] M. C. Smith and S. Willenbrock, Phys. Rev. **D54**, (1996) 6696.

[7] T. Stelzer, Z. Sullivan and S. Willenbrock, Phys. Rev. **D56** (1997) 5919.

[8] T.P. Tait, Phys. Rev. **D61** (2000) 034001.

[9] A.S. Belyaev and E.E. Boos, Phys. Rev. **D63** (2001) 034012.

[10] M. Fischer et al., Phis. Lett. **B451** (1999) 406. M. Fischer et al., hep-ph/0101322.

[11] S. Willenbrock and D.A. Dicus, Phys. Rev. **D34**, (1986) 155.

[12] M. Jeżabek and J.H. Kühn, Nucl. Phys. **B320** (1989) 20.

[13] J.H. Kühn, hep-ph/9707321, and references therein.

[14] A.Pukhov et al., Preprint SINP MSU 98-41/542, hep-ph/9908288.